

Supporting Information for

A Novel Lyotropic Liquid Crystal Formed by Triphilic Star-Polyphiles: Hydrophilic/Oleophilic/Fluorophilic Rods Arranged in a 12.6.4. tiling

L. de Campo, T. Varslot, M. Moghaddam, J. J.K. Kirkensgaard, K. Mortensen and S.T. Hyde*

Estimated parameters used for the calculation of Invariants and setup of the model structures

The calculations of density (Table 1), volume fractions and SLDs are based on density estimates of the constituent molecular parts from bulk densities (see Table 2a-d).

The scattering length density SLD can be calculated via

$$SLD = \frac{\sum_i b_{c_i}}{V_m}$$

where b_{c_i} is the bound coherent scattering length (Table 3) of all i atoms in the molecular part of estimated volume V_m .¹

$$V_m = \frac{Mw}{dN_a}$$

where N_a is the Avogadro number, Mw is the molecular weight and d the estimated density of the molecular part.

Table 1. Molecular weight and Estimated Density for Surfactants and Star-Polyphiles

	Molecular weight [g/mol]	Estimated Density [g/ml]
B-O ₇ -(H ₁₆) ₂	897.33	0.91
B-O ₇ -H ₁₆ -F ₁₀	1233.08	1.19
B-O ₇ -H ₁₄ -F ₈	1105.01	1.15

Table 2a. Estimated Density, SLD and volume fraction for the surfactant B-O₇-(H₁₆)₂

B-O ₇ -(H ₁₆) ₂	B	H ₁₆	O ₇
chemical structure	C ₆ H ₃ O ₃	C ₁₆ H ₃₃	C ₁₅ H ₃₁ O ₇
estimated density [g/ml]	1.2	0.773	1.07
estimated SLD [nm ⁻²]	2.71E-04	-3.52E-05	4.86E-05
estimated volume fraction	10.4	59.0	30.6

¹<http://www.ncnr.nist.gov/resources/sldcalc.html>

Table 2b¹. Estimated Density, SLD and volume fraction for the star-polyphile B-O₇-H₁₆-F₁₀

B-O ₇ -H ₁₆ -F ₁₀	B	H ₁₆	O ₇	C ₃ -spacer	F ₁₀
chemical structure	C ₆ H ₃ O ₃	C ₁₆ H ₃₃	C ₁₅ H ₃₁ O ₇	C ₃ H ₆	C ₁₀ F ₂₁
estimated density [g/ml]	1.2	0.773	1.07	0.76	1.80
estimated SLD [nm ⁻²]	2.71E-04	-3.52E-05	4.86E-05	-2.72E-05	3.87E-04
estimated volume fraction	9.9	28.0	29.1	5.3	27.7

Table 2c. Estimated Density, SLD and volume fraction for the star-polyphile B-O₇-H₁₄-F₈

B-O ₇ -H ₁₄ -F ₈	B	H ₁₄	O ₇	C ₃ -spacer	F ₈
	C ₆ H ₃ O ₃	C ₁₄ H ₂₉	C ₁₅ H ₃₁ O ₇	C ₃ H ₆	C ₈ F ₁₇
estimated density [g/ml]	1.2	0.762	1.07	0.76	1.756
estimated SLD [nm ⁻²]	2.71E-04	-3.58E-05	4.86E-05	-2.72E-05	3.77E-04
estimated volume fraction	10.7	27.0	31.6	5.8	24.9

Table 2d. (Estimated) Density and SLDs for the variety of H₂O/D₂O wt/wt mixing ratios used

water	H ₂ O	80/20 H ₂ O/D ₂ O	60/40 H ₂ O/D ₂ O	50/50 H ₂ O/D ₂ O	40/60 H ₂ O/D ₂ O	20/80 H ₂ O/D ₂ O	D ₂ O
estimated density [g/ml]	0.998	1.018	1.039	1.049	1.060	1.083	1.107
estimated SLD [nm ⁻²]	-5.59E-05	7.18E-05	2.05E-04	2.73E-04	3.43E-04	4.88E-04	6.38E-04

Table 3. Coherent atomic scattering cross sections for neutrons

Scattering Cross Sections	C	O	H	D	F
b_{c_i} [fm]	6.646	5.803	-3.739	6.671	5.654

Figure S0:

SAXS from the star-polyphile hexagonal phase containing B-O₇-H₁₆-F₁₀ measured using our lab SAXS.

Due to the width and length of the primary beam, only the first 3 peaks are resolved.

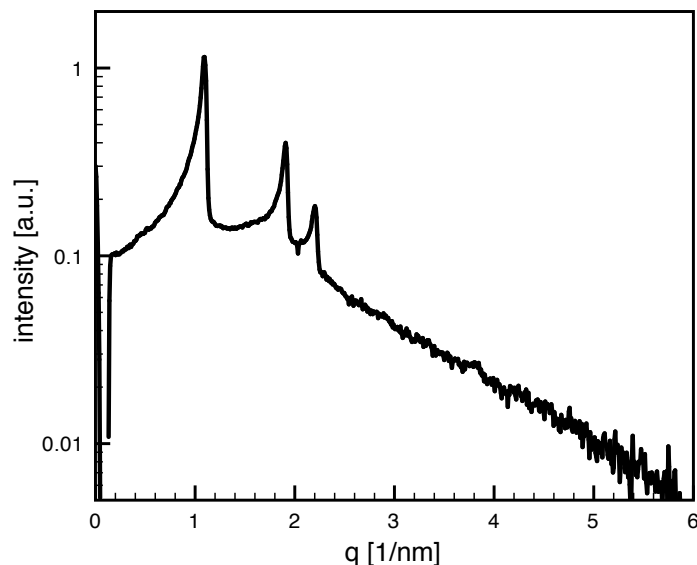


Figure S1:

Porod plot for SANS-data on B-O₇-H₁₆-F₁₀ with 25% D₂O.

To determine the Invariant accurately, it is crucial to determine and subtract the (incoherent) background precisely. This necessitates measurements with good statistics up to high angles. Under the assumption that the structures investigated have a well-defined and smooth surface, the intensity at high-values drops as q^{-4} (Porod law). This can be fitted as straight line in a Porod plot, and the background can be determined from the slope.

In all our data discussed here, we found a good fit to this law over a wide q -range ($q=3\text{nm}^{-1}$ to $q=7\text{nm}^{-1}$), suggesting that most interfaces are indeed well-defined and smooth.

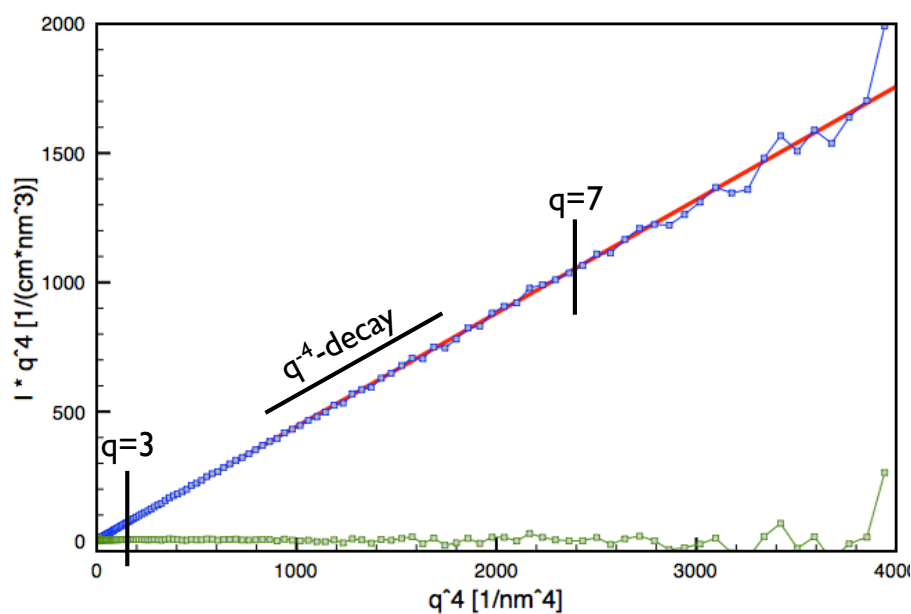


Figure S2:

SWAXS pattern of B-O₇-H₁₆-F₁₀ with 25% water (synchrotron)

X-ray scattering including the wide-angle domains, giving information on local ordering of the molecules. The wide-angle scattering consists of one broad bump for all star-polyphile liquid crystalline samples discussed here. There is no sharp peak that would indicate stacking of the aromatic centers. The broad peak is an overlay of scattering due to hydrocarbon, fluorocarbon and aqueous oligo-ethyleneglycol liquid chain packing.

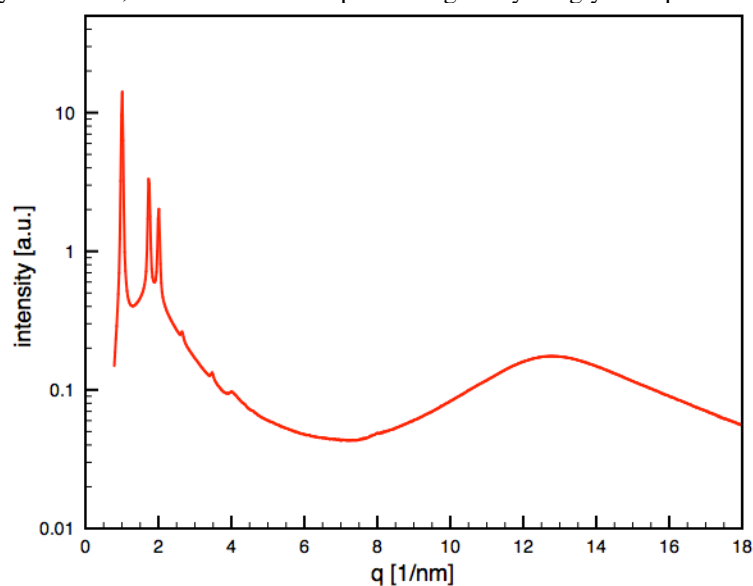


Figure S3:

Effect of Neutron Wavelength Smearing

Simulation of B-O₇-H₁₆-F₁₀ with 25% water (H₂O) assuming a 12.6.4. tiling (case 1)

The typical 10% wavelength spread in SANS causes peaks to decrease in intensity and broaden.

This smearing effect is more pronounced at high angles than at low angles.

Note, however, that it does not alter the value of the Invariant.

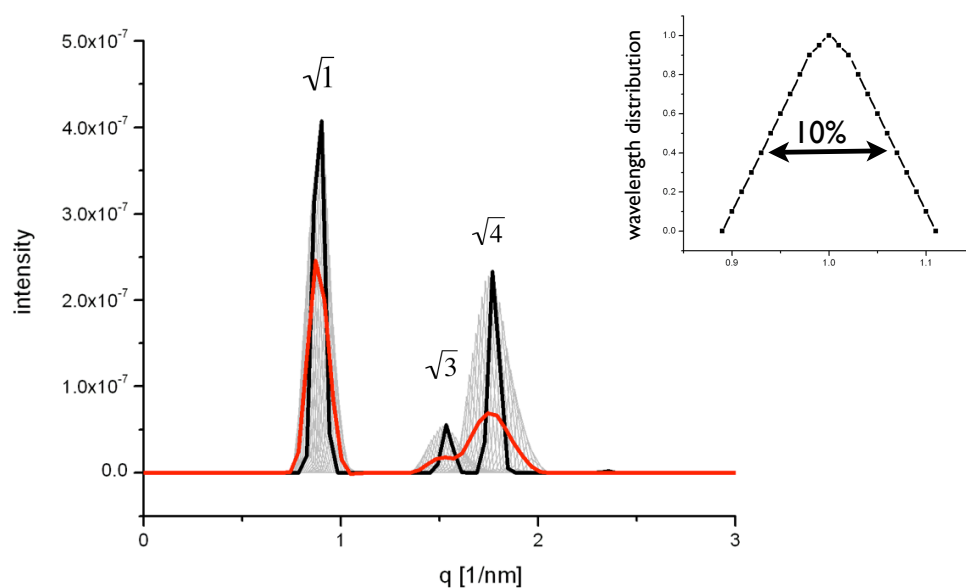


Figure S4.

Additional simulated contrast variations based on the amphiphilic hexagonal phase B-O₇-(H₁₆)₂ with 25% water under the estimated experimental conditions

- a) volume (hydrophilic)=46%, volume (center)=10% (cross section: hexagon)
- b) volume (hydrophilic)=46%, volume (center)=7% (cross section: hexagon)
- c) volume (hydrophilic)=46%, volume (center)=7% (cross section: dodecagon)
- d) volume (hydrophilic)=41% aqueous O-chains + 5% water, volume (center)=7% (cross section: hexagon)

There are only slight differences due to the exact shape of the cross section of the rods (b and c), and due to the width aromatic sheath (a and b). The second peak is always growing. But introducing 5% demixed water in the middle of the hydrophilic channel can cause the second peak to decrease (d).

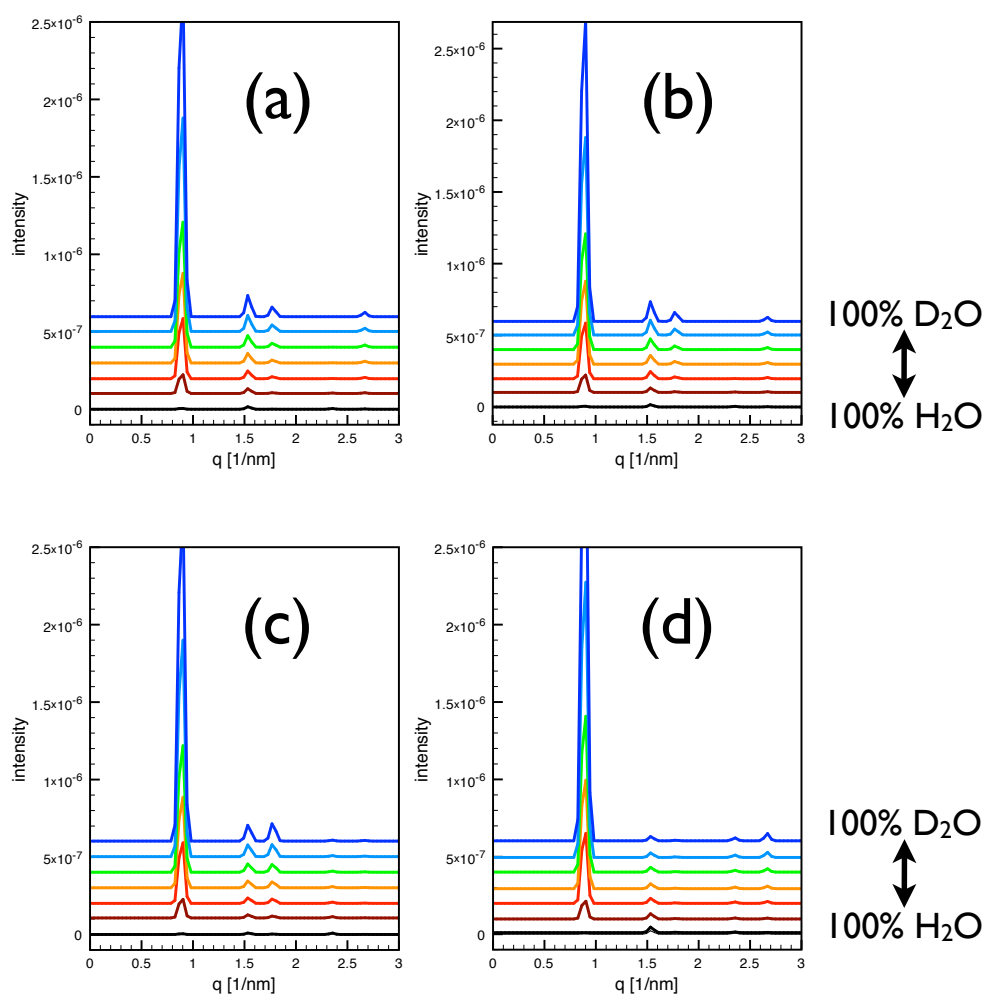


Figure S5:

Additional simulated contrast variations based on 6.6.6. and 12.6.4. tilings under the estimated experimental conditions for B-O₇-H₁₆-F₁₀ with 25% water

- (a) 6.6.6. tiling: volume (hydrophilic)=45%, volume (HC)=27.5%, volume (HC)=27.5%
- (b) 6.6.6. tiling: volume (hydrophilic)=45%, volume (HC)=24%, volume (FC)=24%, volume (center)=7%
- (c) 6.6.6. tiling: volume (hydrophilic)=23%O-chains + 22% water, volume (HC)=24%, volume (FC)=24%, volume (center)=7%
- (d) 12.6.4. tiling: volume (hydrophilic)=46.5%, volume (HC)=28% (hexagons), volume (FC)=25.5% (quadrangles)
- (e) 12.6.4. tiling: volume (hydrophilic)=46.5%, volume (HC)=22% (hexagons), volume (FC)=25% (quadrangles), volume (center)=6.5%
- (f) 12.6.4. tiling: volume (hydrophilic)=46.5%, volume (HC)=28% (hexagons), volume (FC)=25.5% (quadrangles)

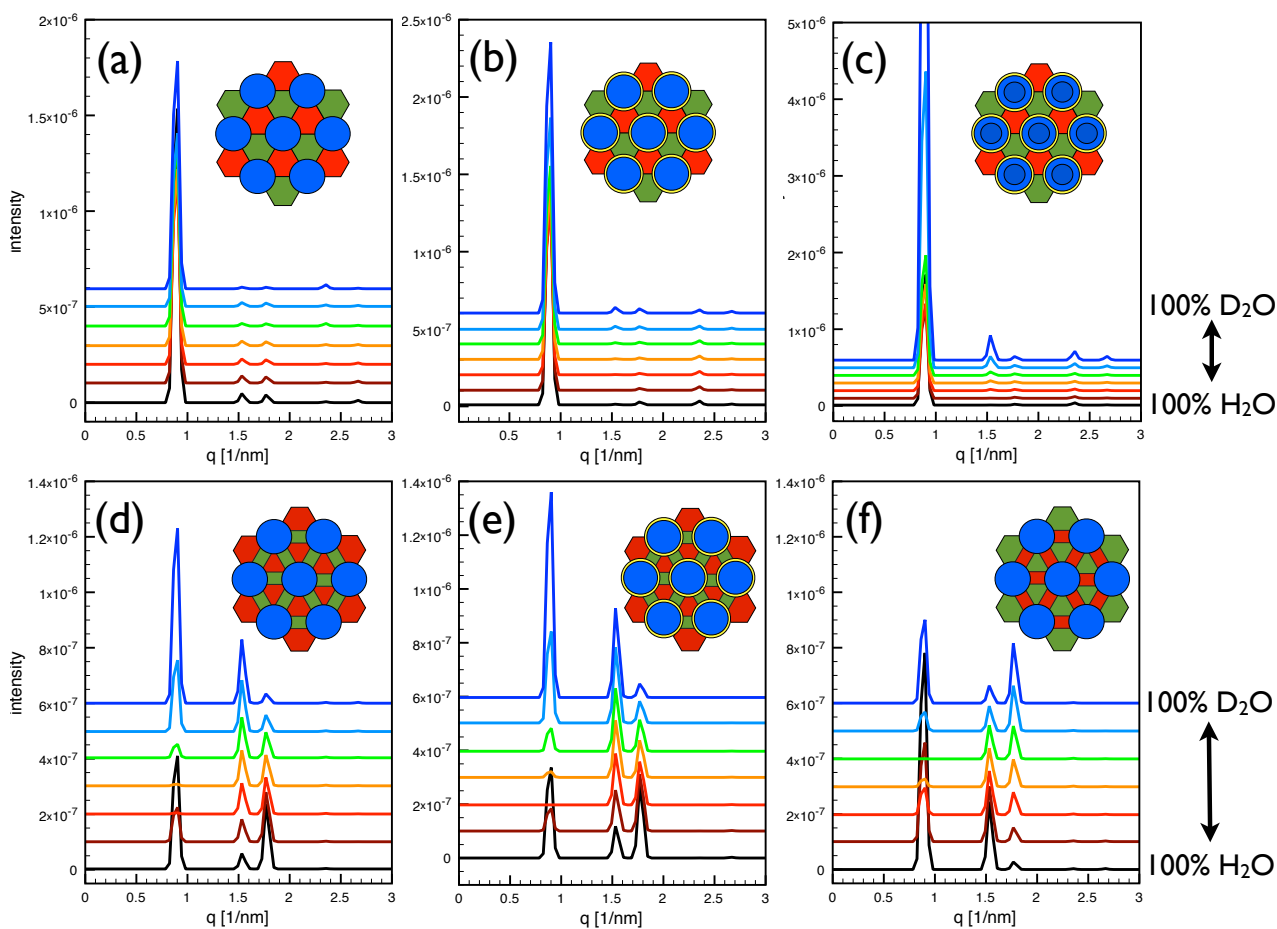


Figure S6:

Simulated contrast variations of 12.6.4 tilings at different volume fractions of the hydrophilic phase

SLD (dodecagons)=-1, -0.5, 0, 0.25, 0.5, 0.75, 1, 1.5, 2

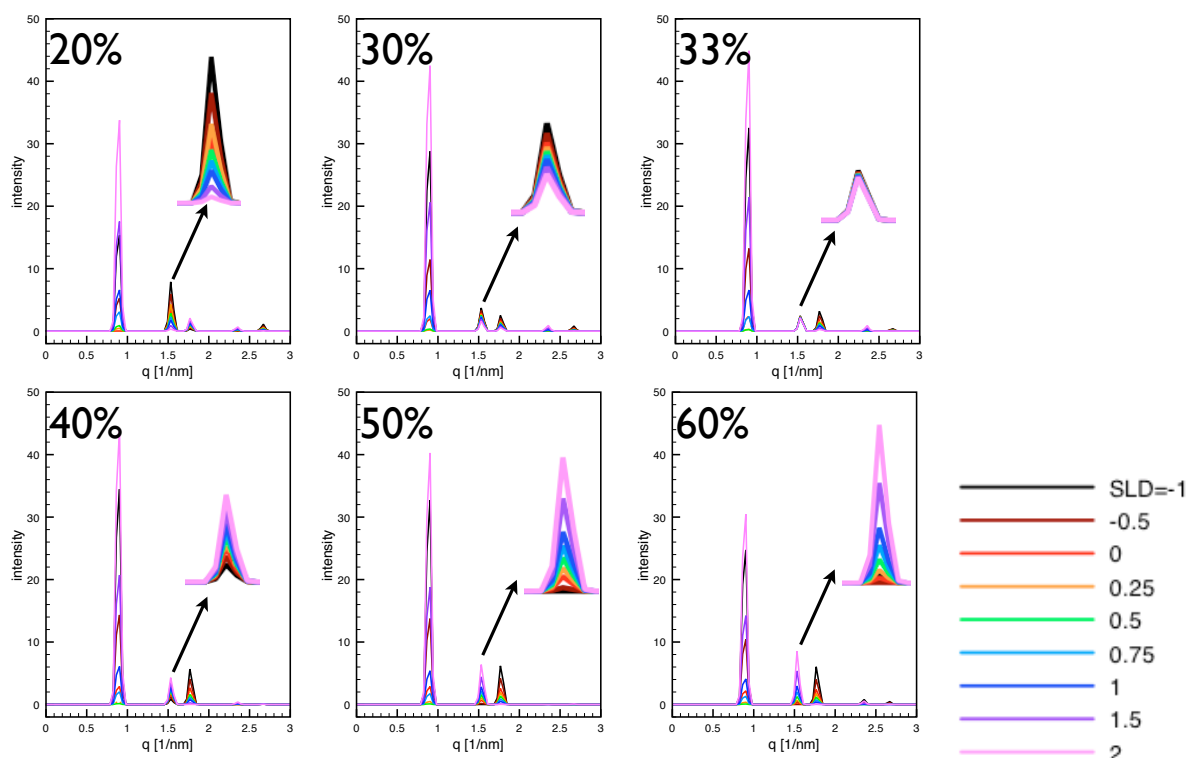
SLD (hexagons)=0

SLD (quadrangles)=1

The volume fractions (quadrangles)=volume fraction (hexagons). The volume fraction of the dodecagons is varied from 20% to 60%.

Conclusion: the hydrophilic volume has not much influence on the first peak, but does influence significantly the second peak. The second peak decreases in such a contrast variation at a hydrophilic volume less than 33% (33% corresponds to H/O/F=1/1/1), while at a higher volume fraction it increases.

Note that the case would be reverse if the SLDs of the hexagons and quadrangles were exchanged.



Summary:

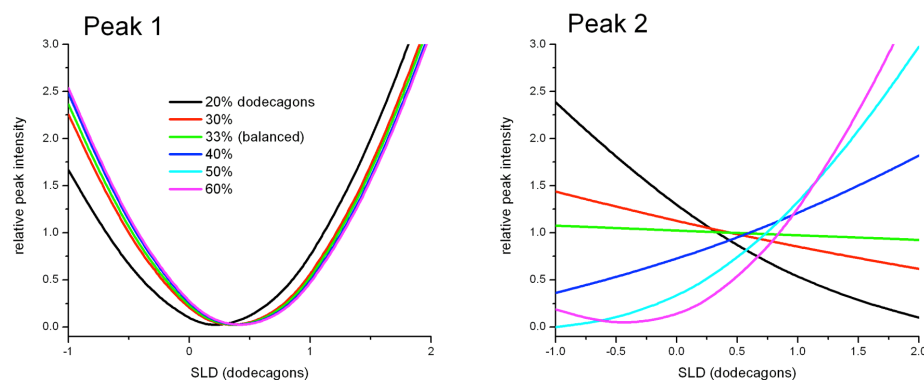


Figure S7:

Simulated contrast variations of 12.6.4 tilings at 40% hydrophilic volume fraction, and varying the volume fraction ratio of the H- and F-domains

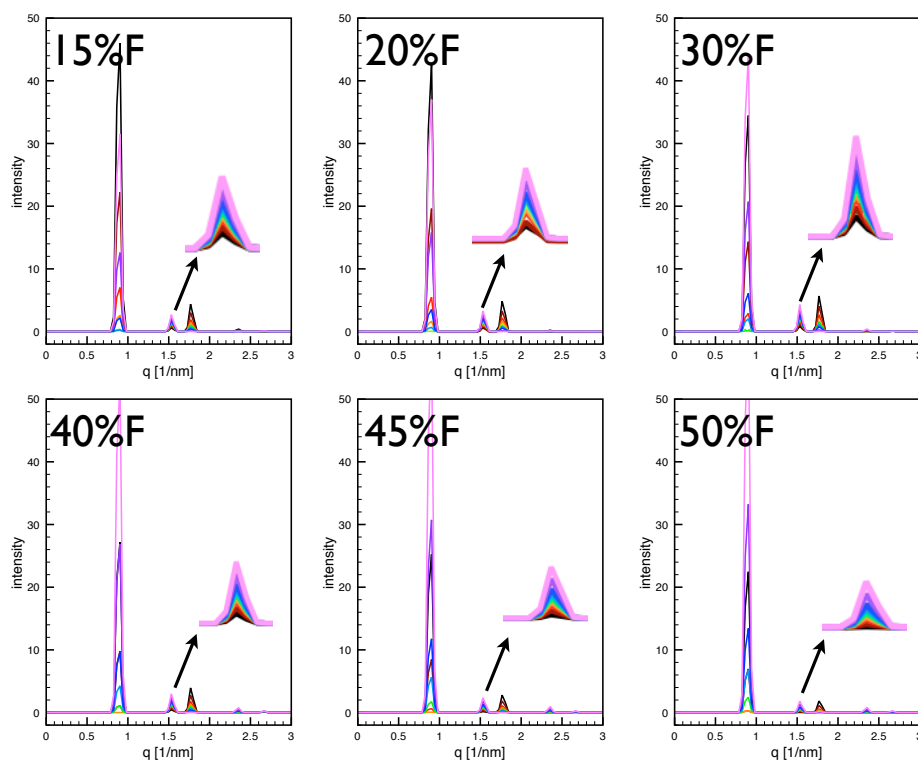
SLD (dodecagons) = -2, -0.5, 0, 0.5, 0.75, 1, 2, 3

SLD (hexagons) = 0

SLD (quadrangles) = 1

At constant volume fraction of the dodecagons (40%), the volume fractions of the quadrangles is varied from 15%F to 50%F.

Conclusion: Unbalancing the H/F volume fraction shifts the position of the minimum of the first peak, but has little impact on the second peak. The second peak is always increasing over a wide H/F ratio.



Summary:

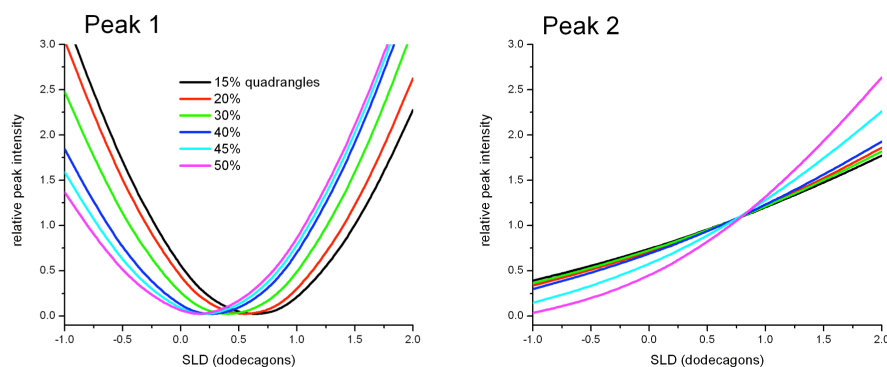


Figure S8:

Simulated contrast variations of 6.6.6. tilings at different volume fractions of the hydrophilic phase

SLD (hexagons) = -2, -1, -0.5, 0, 0.5, 1

SLD (hexagons1) = 0

SLD (hexagons2) = 1

The volume fraction of one set of hexagons is varied from 20% to 60%.

Conclusion: In all these cases, the first peak is much more intense than the second at all contrasts. The scattering patterns are mirrored at an SLD of 0.5. This is also the minimum of the Invariant. At this point, the first peak is small, but always well above zero.

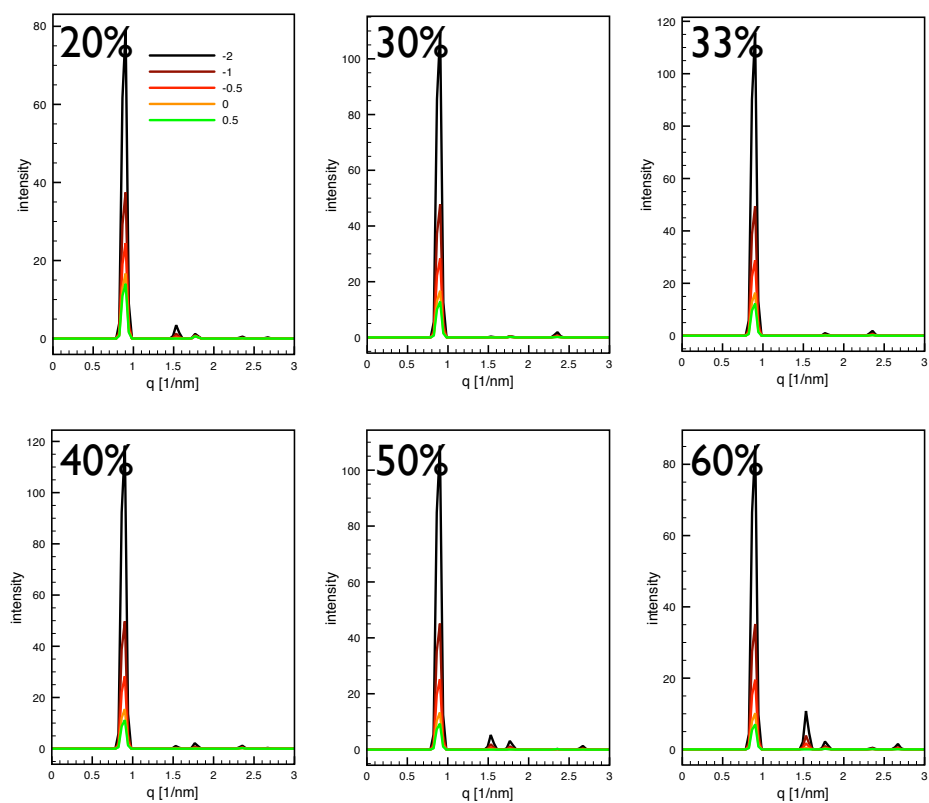


Figure S9:

Simulated contrast variations for an unbalanced 6.6.6. tiling



Volume (hex1)=33

Volume (hex2)=39

Volume (hex3)=27

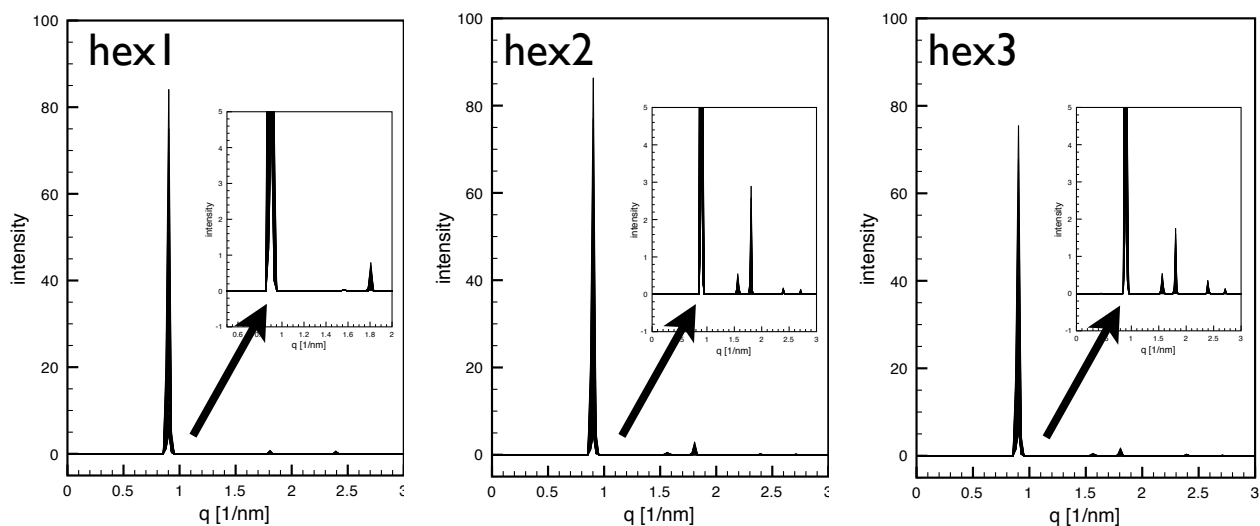
The SLD of one hexagon was varied, while the respective other two were fixed to 0 and 1, respectively.

SLD (hex1) = -3 to 3 in 0.2 steps

SLD (hex2) = 0

SLD (hex3) = 1

Each figure below shows the simulated scattering for the range of SLD-variations within each hexagon. The insets zoom in on weaker intensities.



Conclusion: In common with the balanced case, unbalanced 6.6.6. tilings give rise to a first peak that is more intense than the second at all contrasts.